Shear Strengthening Effects with Varying Types of FRP Materials and Strengthening Methods

by J. Sim, G. Kim, C. Park, and M. Ju

Synopsis: The FRP system is a good alternative of the traditional shear strengthening technique. This study evaluates the shear strengthening effects on the reinforced concrete beams strengthened with varying types of FRP materials, CFRP, CFS and GFRP. The entire strengthened specimens were failed in the mode of brittle shear failure with debonding of the FRP materials. The shear capacities were improved mostly by more than 54%. The different types of the strengthening materials did not yield a noticeable difference in the shear strengthening effect. The orientation of the fibers, however, was found to be an important factor. With a 45° fiber orientation, greater strengthening effect and better control on the shear crack propagation were observed. A numerical model predicting the shear capacity of the shear-strengthened beams was suggested along with the strength efficiency factor from the test results. The predictions were in good agreement with the test results.

1666 Sim et al.

ACI Member **Jongsung Sim** is a professor at the department of civil and environmental engineering at Hanyang University, Ansan, Korea since 1987. He obtained his Ph. D. degree from Michigan State University. His primary research area includes reinforced concrete structures, fiber reinforced polymer materials, repair and rehabilitation of concrete structures and recycling of waste concrete.

Gyuseon Kim is a deputy chief of the division of bride inspection at Korea Infrastructure and Safety and Technology Corporation. He obtained his Ph.D. degree from Hanyang University, Seoul, Korea in 2000.

ACI Member **Cheolwoo Park** is a research professor at the department of civil and environmental engineering at Hanyang University, Ansan, Korea. He obtained his Ph.D. degree from the University of Illinois at Urbana-Champaign, USA in 2001. His primary research area includes reinforced concrete structures, fiber reinforced polymer materials, repair and rehabilitation of concrete structures and recycling of waste concrete.

Minkwan Ju is a Ph.D. candidate at the department of civil and environmental engineering at Hanyang University, Ansan, Korea.

INTRODUCTION

Reinforced concrete beam members are designed to fail in a ductile manner under ultimate loading condition. In order to assure the ductile failure in flexure, however sufficient shear capacity should be necessarily provided. This principle will be conceptually applied to the repair or strengthening of damaged concrete structures as well Steel plate bonding system or section enlargement has been a typical shear strengthening technique. As an alternative to traditional techniques, the strengthening using fiber reinforced polymer (FRP) systems has emerged. This system provides advantages over the traditional technique: lightweight, relatively easy installation and non-corrosiveness[1-4] Most common FRP materials among a variety of kinds may include carbon fiber reinforced polymer (CFRP), carbon fiber sheet (CFS), and glass fiber reinforced polymer (GFRP). The products of these materials may be available in various forms with different fiber volume, resin matrix, fiber orientation, and dimension. Those factors play an important role in establishing the characteristics of FRP materials and hence the FRP strengthening systems. This study investigates the shear-strengthening effects and the behaviors of concrete beams strengthened with CFRP, CFS and GFRP. Several different methods were involved in the installation of the materials. By using the test results and the concrete plasticity theories[5-9], a modified numerical model is also suggested for predicting the shear capacity of the shear-strengthened concrete beams.

EXPERIMENTS

Materials and specimen fabrication

Beam specimens were fabricated with 24MPa strength concrete and with two different sizes of reinforcing bars, No. 4 and 5, of 400MPa yielding strength. Table 1 and Figure 1 describe the concrete mix proportion and the details of specimen geometry, respectively. In order to account for the purpose of this study, the beam specimens were designed to be under-reinforced for shear. Assuming the beam would fail in the mode of flexure, the calculated flexural strength of the non-strengthened beam was 193KN, which was about twice greater than the shear capacity under the given loading configuration shown in Figure 1. Therefore, the specimens were expected to fail in the mode of shear rather than flexure.

The strengthening materials used in this study were CFRP, CFS and GFRP and Table 2 addresses the physical properties of these materials. In the design of strengthening, a strengthening method may vary according to the material characteristics. Sides wrapping or stripping method is one of the typical methods for CFRP due to the thickness of its products. CFS and GFRP are relatively flexible and easy to handle so that sides or complete wrapping methods are usually applied. In this study, those typical strengthening methods were applied and the methods were designated as S, II, and U for stripping, sides wrapping and complete wrapping, respectively, as described in Table 3. In the II strengthening method, two different fiber orientations were considered, 45° and 90° but only 90° in the U method. The strips of CFRP were installed in the angle of 45° and 90° from the longitudinal rebar. Figure 2 schematically depicts the applied strengthening methods.

Tests

In the beam shear tests, vertical load was applied statically by using a 2,000 kN testing machine under a four–point loading configuration with the shear span-to-depth ratio, a/d, of 1.7. The mid-span deflection was measured at the bottom of the specimen. The strains of the strengthening materials and the bottom rebar were measured using strain gages. Location of the stain gages attached on the strengthening materials was away for the distance of the approximate effective depth from the supports. While load was being applied, the deflection and strains were measured simultaneously.

RESULTS AND ANALYSIS

Failure mode

The entire specimens were failed in the mode of shear failure and no yielding of reinforcing steel was measured. The specimens strengthened with CFRP exhibited a brittle failure with the debonding of CFRP from the surface of concrete. In the CP45S specimen where CFRP was strengthened by stripping with an angle of 45°, cracks initiated at the loading area and propagated vertically to the bottom. This is not a typical diagonal shear cracking pattern and implies that the crack propagation was effectively

controlled by 45° CFRP stripping strengthening. The specimens strengthened with CFS and GFRP experienced the diagonal shear cracking patterns and the strengthening materials were torn at the angle perpendicular to the fiber orientations, followed by the debonding of the strengthening materials. In the specimens strengthened with CFS, more pieces of concrete were broken apart from the surface with the debonding of the strengthening materials comparing to the specimens strengthened with CFRP and GFRP. Figure 3 shows the observed typical cracking patterns of the tested specimens.

Load-strains of strengthening materials

The strengthening materials used in this study held only one orientation and consequently, physical meanings were given only to the strains corresponding to the fiber orientation. Figure 4 shows the measured load-strain behaviors and the strains at failure are summarized in Table 3. The strains were not significantly increased up to the failure in most specimens, followed by instantaneous increase at failure. This observation well coincides with the brittle failure mode. However, some degree of gradual increase was observed in the specimens strengthened with CFRP stripping. For this phenomenon, three hypotheses may be available: first, the geometry of the stripping has different restraining effect on cracking; second, the thicker section of CFRP with resin matrix has different tensile behavior; and third, the combined interaction of both.

Strengthening effects

The measured load-deflection behaviors are shown in Figure 5. In the entire specimens, the applied load immediately decreased after the maximum shear capacity. This sudden decrease of the shear capacity or brittle failure mode was primarily due to the debonding of strengthening materials as cracks developed in concrete. In Figure 5, it was noted that the specimens strengthened with CFRP demonstrated variations of the flexural stiffness with respect to the strengthening methods while other specimens showed very consistent stiffness. This might be because of the modification of the flexural stiffness of the beams since the CFRP products used in this study were relatively thick comparing to other strengthening materials. Yet, the measured shear capacity was similar to other specimens.

The strengthening effect was defined as a ratio of the measured maximum applied load of the non-strengthened to the strengthened specimen. As shown in Table 3, the strengthening effects were ranged between 54.8% and 73.3% except for the CS90U specimen. In the CS90U specimen demonstrated a quite low strengthening effect, it was believed by the authors that there might have been problems in the bonding process of CFS onto the concrete surfaces. In the test results, the different strengthening methods did not yield a certain relationship to the strengthening effect. The orientation of the fibers, however, was found to be an important factor. When the fiber orientation was 45°, the strengthening effect was improved by more than 10% in each case comparing to 90°. From this observation, it may be concluded that the strengthening effect is more relevant to the fiber orientation rather than the strengthening materials or methods. Also, greater attention should be given in the fiber orientation during the installation of the FRP materials. As mentioned earlier, since the specimens strengthened with CFS showed

tearing of fibers in the direction perpendicular to the fiber orientation, it is anticipated that better shear strengthening may be achieved if the number of fibers, i.e., layer of CFS, is increased. It should be noted that, however, the strengthening with CFS or GFRP may hinder engineers from crack inspection with the wrapping method while the strengthening with CFRP stripping at 45° can provide better visibility for later crack inspection. More efficient strengthening methods with respect to each different strengthening material may be sought with further researches.

SHEAR CAPACITY PREDICTION MODEL AND ANALYSIS

Model

This study suggests a numerical model for predicting the shear capacity of strengthened reinforced concrete beams. When the beams are under combined mode of flexure and shear, the truss model proposed by Thurlimann[11] could be more appropriately applied. The specimens in this study, however, were assumed to be under the shear only mode with a/d ratio of 1.7 and hence the model suggested in this study was based on the study of Nielson and Braestrup[9], in which the problem was solved by means of the upper-bound solution techniques with the limit theory of perfect plasticity.[11]   Figure 6 shows an idealized failure mechanism of the shear-strengthened beam where only the middle part, indicated as (A), is subjected to the vertical deflection, u, and no deflection is occurred in the outside parts, indicated as (B). Between the parts (A) and (B), a straight yield line is also assumed with an angle of θ. Applying the energy conservation theory, the equilibrium is expressed as below.

$$V \cdot u = V_{sp} \cdot u + V_c \cdot u = \left[\left(s_y + \alpha \cdot \gamma_y \right) bd \cot \theta \right] \cdot u + \left[\frac{1}{2} v \cdot \sigma_{cu} \left(1 - \cos \theta \right) \frac{bd}{\sin \theta} \right] \cdot u \qquad (1)$$

where, $s_y = \dfrac{A_v \cdot f_{sy}}{b \cdot e}$, $\gamma_y = \dfrac{A_p \cdot f_{py}}{b \cdot t} \left(\sin \beta + \cos \beta \right)$, β = angle between beam and

strengthening material, σ_{cu} = concrete compressive strength, d = effective depth of beam, A_v, A_p = cross sectional area, f_{sy}, f_{py} = yield strength, e, t = spacing of stirrup and strengthening material, respectively, V_{sp} = combined shear capacity of stirrup and strengthening materials, and V_c = shear capacity of concrete. On the right hand side of Eq. (1), the first term represents the work done by stirrup and strengthening material corresponding to the deflection, u, and the second term by concrete. v is a constant that represents the contribution of compressive strength of concrete. This constant shall be less than 1.0 because the concrete stress in the web does not reach to the concrete compressive strength, σ_{cu}. There may be several reasons including the uncertainty at failure, the limited deformation of concrete, and complicated bonding/slip behavior between concrete and rebar. In the study herein, v was decided to be 0.4 concerning the fact that the width of the beam specimen was relatively large comparing to the depth.[12] In addition, since the strengthening materials in this study were not embedded in the body of concrete, the strength of the strengthening materials would not be completely participated in shear-strengthening. Therefore, this study suggest to use a strength efficiency factor, α, that can be obtained from the test results. The factor, α, should be

highly dependant on the physical characteristics of strengthening materials, bonding between concrete and strengthening materials, and strengthening methods. Eq. (1) can be rewritten as below with appropriate mathematical implementations.

$$\frac{\tau}{v\sigma_{cu}} = \phi\cos\theta + \frac{1}{2}[\sqrt{(1+\cot^2\theta)} - \cot\theta]$$
(2)

where, $\tau = \dfrac{V}{b\cdot h}$, $\phi = \phi_1 + \alpha\cdot\phi_2$, $\phi_1 = \dfrac{A_v\cdot f_{sy}}{b\cdot e\cdot v\sigma_{cu}}$, and $\phi_2 = \dfrac{A_p\cdot f_{sy}}{b\cdot t\cdot v\sigma_{cu}}(\sin\beta + \cos\beta)$.

The value of θ satisfying the least-upper bound solution can be found by applying the fact that the derivative of V with respect to θ becomes 0. Then Eq. (2) becomes

$$\tan\theta = \frac{2\sqrt{\phi(1-\phi)}}{1-2\phi}$$
(3)

which leads to the least-upper-bound solution that is the shear capacity of the shear-strengthened beam

$$\frac{\tau}{v\sigma_{cu}} = \sqrt{\phi(1-\phi)}$$
(4)

The limit values are determined depending on θ which, for geometrical reasons, must be in the range

$$\frac{a}{d} \le \tan\theta \le \infty \quad\text{or}\quad 0 \le \cot\theta \le \frac{a}{d}$$
(5)

Equation (6) below is the final product and can be used to predict the shear capacity of shear-strengthened beams as long as the a/d ratio is less than 2.0 where the shear failure is governing.

$$\frac{\tau}{v\sigma_{cu}} = \frac{\sqrt{a^2+d^2} - (1-2\phi)a}{2d} \quad\text{if } \phi < \frac{\sqrt{(a^2+d^2)} - a}{2\sqrt{(a^2+d^2)}} = \lambda$$
(6, a)

$$\frac{\tau}{v\sigma_{cu}} = \sqrt{\phi(1-\phi)} \qquad\text{if } \lambda \le \phi \le \frac{1}{2}$$
(6, b)

$$\frac{\tau}{v\sigma_{cu}} = \frac{1}{2} \qquad\text{if } \phi > \frac{1}{2}$$
(6, c)

Analysis and discussion

      In this study, the strength efficiency factor, α, was calculated by substituting the shear capacity of the control specimen into V_c in Eq. (1). Then the obtained α values for each strengthening material were averaged as described in Table 3. These α values take strengthening characteristics of each material into account. Using the obtained α, the shear capacity of the specimens was calculated and the results are summarized in Table 4.

In general, the predicted shear capacities were in good agreement with the measured values. In order to evaluate the validity of the model proposed herein, the model was applied to the extensively collected test data in the study of Chen and Teng.[13] In order to compare the shear strengthening effect from the FRP materials, V_{sp} neglecting the contribution of stirrups, s_y, in Eq. (1) was compared with the V_{frp} in [13]. The contributions of FRP to shear strength predicted by the proposed model and other test data provided in [13] were very comparable each other as shown in Figure 7, which indicates a potential applicability of the model that associated with the strength efficiency factor, α. From these observations, it can be concluded that the model suggested in this study may be successfully used for predicting the shear capacity of the shear-strengthened beams with FRP materials. The strength efficiency factor, α, however, is a function of other physical and geometric factors including the characteristics of strengthening materials, bonding properties, and a/d ratio, etc. It is, therefore, anticipated that more reliable prediction model may be obtained provided more variables are concerned in further study.

CONCLUSIONS

This study evaluated the shear-strengthening effects of the reinforced concrete beams with varying types of FRP materials, CFRP, CFS and GFRP. From the test results, a model predicting the shear capacity of the shear-strengthened beams was suggested. From the studies presented herein the following conclusions were drawn.

(1) The entire shear-strengthened specimens were failed in the mode of brittle shear failure with debonding of the FRP materials.
(2) The shear capacities of the shear-strengthened beams were improved by more than 54% by applying the FRP materials except for the specimen strengthened with CFS with the 90°-complete wrapping method. The different types of the strengthening materials did not yield a noticeable difference in the shear strengthening effect.
(3) The orientation of the fibers was found to be an important factor. With a 45° fiber orientation, greater strengthening effect and better control on the shear crack propagation could be achieved.
(4) In the specimens strengthened with CFS, failure occurred as tearing of the sheets in the direction perpendicular to the fiber orientation. Better shear strengthening may be possible provided the number of CFS layer is increased.
(5) When further crack inspection is expected on the FRP strengthening systems, the stripping method may be recommended as long as the sufficient strengthening effect is provided.
(6) A model predicting the shear capacity of the shear-strengthened beams was suggested along with the strength efficiency factor. The results were in good agreement with the test results herein and in other studies. For more reliable model, however, further studies involving more variables should be necessary.

REFERENCES

1. "Guide for the Design and Construction of Externally Bonded FRP Systems for Strengthening Concrete Structures," ACI 440.2R-02, Reported by ACI Committee 440, American Concrete Institute, Farmington Hills, MI, USA.

2. Al-Sulaimani, G. J., Sharif , A., Basunbul, I. A. , Baluch, M. H. and Ghaleb, B. N., 1994, "Shear Repair for Reinforced Concrete by Fiberglass Plate Bonding," *ACI Structural Journal*, Vol. 91, No. 4, pp. 458-464.

3. Taljsten, B., 1995, "Strengthening of Structures Using Epoxy Bonded Steel or Fibre Reinforced Plastic Plates," Extending the Lifespan of Plastic Plates, IABSE Symposium, San Francisco, Vol. 73, pp. 1173-1179.

4. "An Experimental Study on Repair and Rehabilitation Methods for Deteriorated Concrete Structural Members," Technical Report submitted to the Korea Highway Corporation, 1996, pp. 161-167.

5. Braestrup, M. W., 1974, "Plastic Analysis of Shear in Reinforced Concrete," *Magazine of Concrete Research*, Vol. 26, No. 89, pp. 221-228.

6. Campbell, T. I., Chitnuyanondh, L., and de V. Batchelor, B., 1980, "Rigid-Plastic Theory V. Truss Analogy Method for Calculating the Shear Strength of Reinforced Beams," *Magazine of Concrete Research*, Vol. 32, No. 110, pp. 39-44.

7. Efrosini Drimoussis et al, "Shear Strengthening of Concrete Bridge Girders using Carbon Fiber-Reinforced Plastic Sheets," Fourth International Bridge Engineering Conference, pp. 337-347.

8. Lim, T. Y. and Lee, S. L., 1987, "Shear and Moment Capacity of Reinforced Steel-Fibre-Concrete Beams," *Magazine of Concrete Research*, Vol. 39, No. 140, pp. 148-160.

9. Nielsen, M. P. and Braestrup, M.W., 1975, "Plastic Shear Strength of Reinforced Concrete Beams," *Bygningsstatiske Meddelelser*, Vol. 46, No. 3, pp. 61-99.

10. Thurlimann, B., 1974, "Plastic Analysis of Reinforced Concrete Beams," IABSE Colloquium on Plasticity in Reinforced Concrete, Introductory Report, Bangkok, Thailand,   Vol. 26, No. 89, pp. 221-228.

11. Chen, W. F., 1982, Plasticity in Reinforced Concrete, McGraw-Hill, USA.

12. Taylor, R., 1963, "Some Aspects of the Problem of Shear in Reinforced Concrete Beams," *Civil and Public Works Review*, Vol. 58, pp. 629-632.

13. Chen, J. F. and Teng, J. G., 2003, "Shear capacity of FRP-strengthened RC beams: FRP debonding," *Construction and Building Materials*, Vol. 17, pp. 27-41.

Table 1 — Concrete mix proportion

Cement (kg/m^3)	Water (kg/m^3)	F. A. (kg/m^3)	C. A. (kg/m^3)	w/c (%)	S/a (%)
371	182	826	909	49	47.6

Table 2 — Physical properties of strengthening materials

Materials	Tensile strength (MPa)	Elastic modulus (MPa)	Specific Gravity	Elongation (%)
CFRP	3,160	1.6×10^5	1.60	1.9
CFS	3,500	2.4×10^5	1.62	1.5
GFRP	450	2.3×10^4	1.15	2.0

Table 3 — Specimens and test results

Specimens	Description		Failure load (kN)	Strengthening effect (%)	ε of FRP at failure ($\times$ E^{-6})
	Materials	Method			
CON	Control		105	-	-
CP90II	CFRP	90° sides	173	64.8	366
CP90S		90° strip	163	54.8	1,890
CP45S		45° strip	178	69.0	2,123
CS90II	CFS	90° sides	170	61.9	50
CS45II		45° sides	182	73.3	130
CS90U		90° complete	133	26.7	51
GP90II	GFRP	90° sides	168	60.0	211
GP45II		45° sides	180	71.4	25
GP90U		90° complete	177	68.6	56

Table 4 — Strength efficiency factor, α

Materials	CFRP	CFS	GFRP
α	0.039	0.232	0.340

Table 5 —Predicted shear capacities

Specimens	Experimental results (kN)	Predicted results (kN)			Predicted / Experimental (%)
		V_{sp}	V_c	$V_{sp} + V_c$	
CON	105	-	115.8	115.8	110
CP90II	173	96.1	115.8	211.9	122
CP90S	163	48.1	115.8	163.9	101
CP45S	178	67.9	115.8	184.7	104
CS90II	170	59.5	115.8	175.3	103
CS45II	182	84.2	115.8	200.0	110
CS90U	133	59.5	115.8	175.3	132
GS90II	168	60.4	115.8	176.3	105
GS45II	180	85.4	115.8	201.3	112
GS90U	177	60.4	115.8	176.3	100
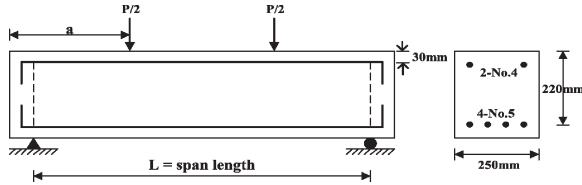
Figure 1 — Specimen geometry and loading scheme (a/d = 1.7)
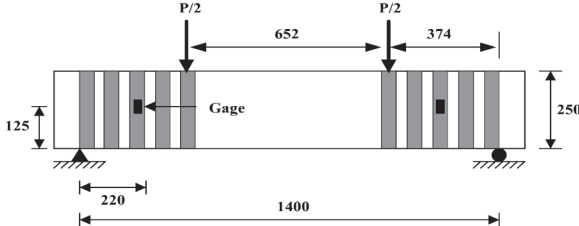
(a) 90° stripping (unit: mm)
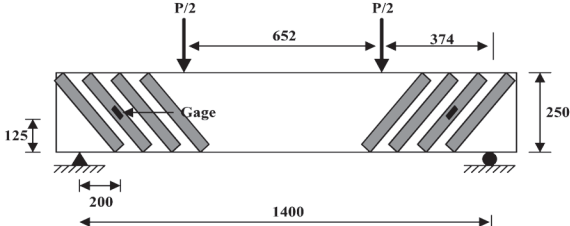
(b) 45° stripping (unit: mm)
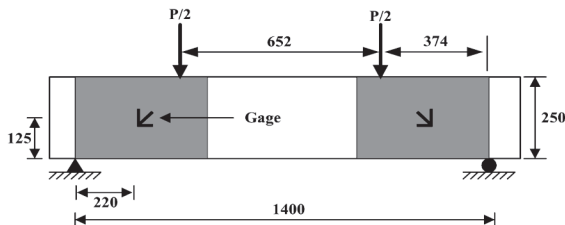
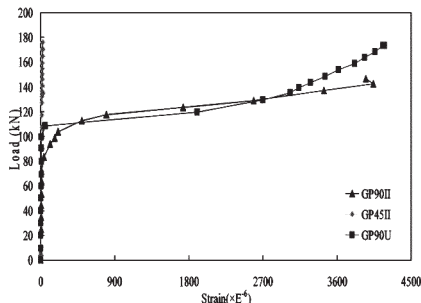(c) II, U wrapping (unit: mm)

Figure 2 — Strengthening methods

(a) Control (CON)

(b) 90° strip (CP90S)

(c) 45° strip (CP45S)

(d) 90° complete (CS90U)

(e) 45° complete (GP45II)
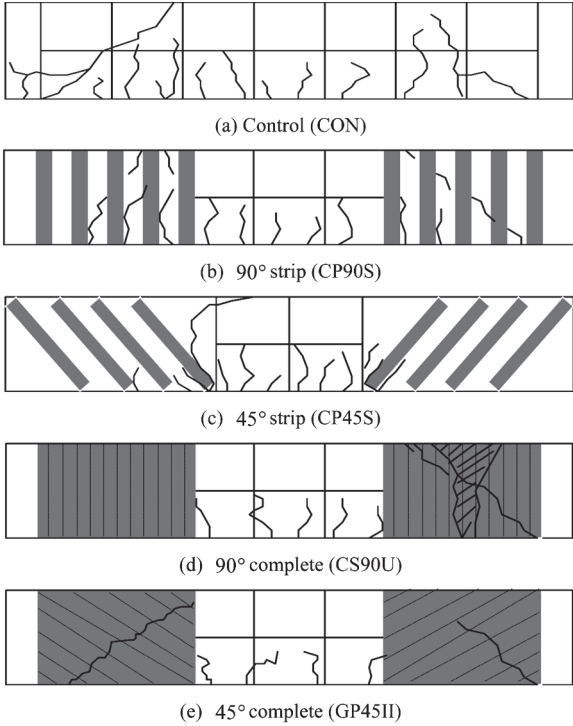
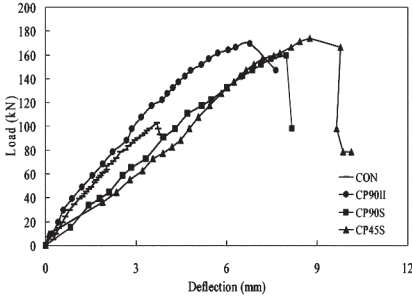Figure 3 — Cracking patterns of tested specimens
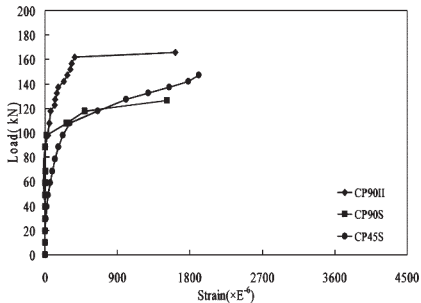
(a) CFRP
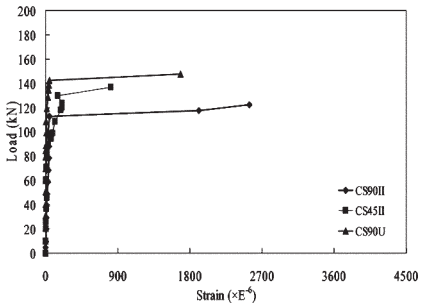
(b) CFS

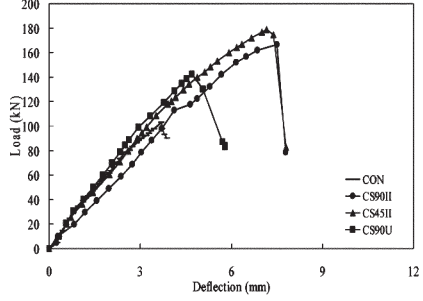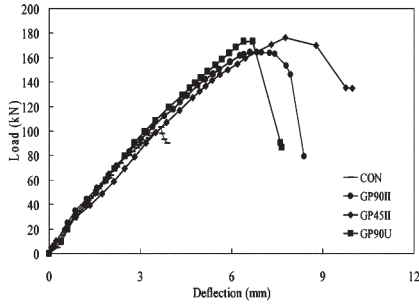(c) GFRP

Figure 4 — Load-strain of FRP strengthening materials

(a) CFRP

(b) CFS

(c) GFRP
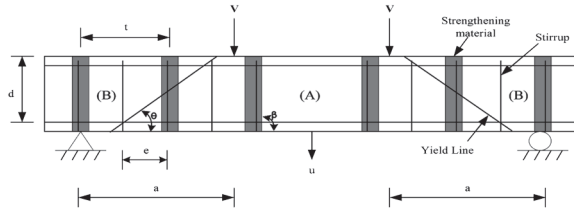
Figure 5 — Load-deflection behaviors

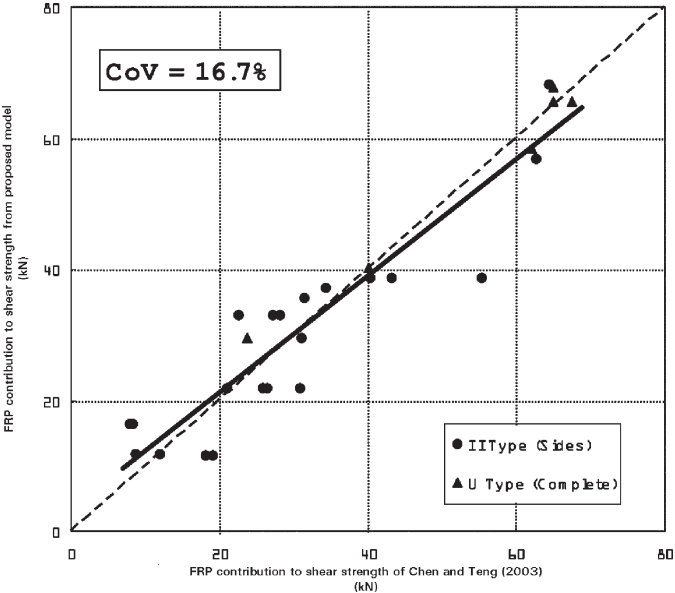Figure 6 — Failure mechanism of RC beam shear-strengthened by FRP

Figure 7 — Comparison of proposed model with other test data

1680 Sim et al.